Journal of Physics: Conference Series

PAPER • **OPEN ACCESS**

Experimental study of three in-line bubbles rising in still water by means of a three-dimensional (3D) shadowgraphy technique

To cite this article: Nunno F Di *et al* 2021 *J. Phys.: Conf. Ser.* **1977** 012002

View the article online for updates and enhancements.

You may also like

- Bubble Manipulation by Self Organization of Bubbles inside Ultrasonic Wave
Yoshiki Yamakoshi and Masato Koganezawa
- Simulation of bubbles motion side by side in lifting pipe of two-stage bubbles pump
Bingbing Liu, Shaojun Zhang and Yue Li
- Three-Dimensional Numerical Coupling Simulation of Two-Phase Flow and Electrochemical Phenomena on Alkaline Water Electrolysis
Kenjiro Torii, Manabu Kodama and Shuichiro Hirai

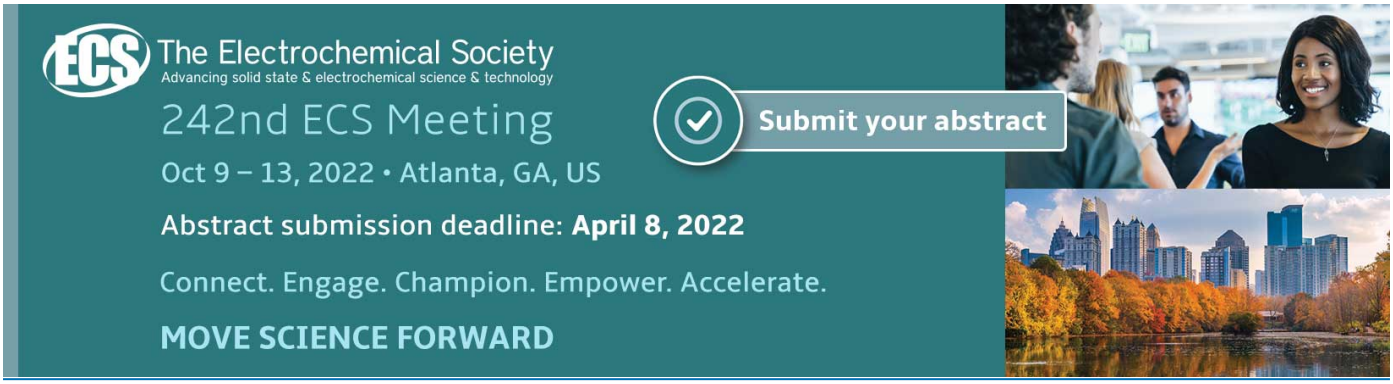

This content was downloaded from IP address 193.205.61.74 on 24/03/2022 at 11:14

Experimental study of three in-line bubbles rising in still water by means of a three-dimensional (3D) shadowgraphy technique

F Di Nunno[1], F Granata[1], M Miozzi[2], R Gargano[1], G de Marinis[1], F Alves Pereira[2], and F Di Felice[2]

[1] Department of Civil and Mechanical Engineering, University of Cassino and Southern Lazio, Cassino, Italy
[2] Institute of Marine Engineering, National Council of Research, Rome, Italy

fabio.dinunno@unicas.it

Abstract.

The dynamics of rising bubbles in still water can be influenced by the wake characteristics of the neighbouring bubbles. An experimental study was conducted on individual rising bubbles rising in still water by means of volumetric shadowgraphy technique. Results highlighted a phase opposition relationship between the volumes and rising velocities and between the minor semi-axis and the two semi-axes median and major of the three air bubbles. The cross-correlation function applied on the eccentricities of the three bubbles highlighted similar positive peaks but also a negative peak between eccentricities of the second and third bubbles. Frequency spectra of the three bubbles eccentricities exhibited some common features, with peaks around 10 Hz for the first and third bubbles and around 5 Hz for the second and third bubbles. In addition, cross-correlation applied on the rising velocities showed negative correlations between the three bubbles, with each bubble that reduces its rising velocity while another accelerates. The application of the volumetric shadowgraphy allowed a simultaneous measurement of the geometry and rising velocities of the in-line bubbles, leading to identify common and different features among them.

1. Introduction

The dynamics of rising bubbles in still water can be influenced by the wake characteristics of the neighbouring bubbles [1]. In literature, there are different works which investigated the wake effect related to a short distance between adjacent rising bubbles [2], with particular attention on bubbles with small size, lower than 1.2 mm [3, 4], for which the wake effect was quite negligible.

In general, several experimental studies on bubbly flows of different types were performed using intrusive conductive probes, which allow to measure air concentration and bubble velocities based on the air-water electrical resistivity difference [5, 6, 7]. Also non-intrusive optical measurement technique, e.g. Particle Image Velocimetry (PIV), were used for a simultaneous 2D measurement of the two phases in air-water flows [8, 9]. However, an accurate analysis of air bubbles dynamics, which commonly are strongly three-dimensional, has required the development of volumetric techniques, including shadowgraphy, a well-known flow visualization technique that highlights the difference of refractive index at the interface between a body and its surrounding medium [10, 11]. Recently, the results of experimental activities on bubbly flows, and other complex flows in the hydraulic field, were used in combination with machine learning algorithms for the development of forecast models [12, 13].

Content from this work may be used under the terms of the Creative Commons Attribution 3.0 licence. Any further distribution of this work must maintain attribution to the author(s) and the title of the work, journal citation and DOI.
Published under licence by IOP Publishing Ltd

In this work, an experimental investigation on a sequence of three in-line rising bubbles in still water has been performed by means of a volumetric shadowgraphy technique, providing a characterization of the air bubbles, both in terms of velocity and geometric features. Size and shape were obtained by means of a space carving algorithm. The experimental results are presented in order to show the suitability of the shadowgraphy technique to perform a detailed analysis of the wake characteristics related to rising in-line bubbles.

2. Materials and Methods

2.1. Experimental setup and instrumentation

The laboratory model consisted of a steel pipe with a diameter *D* equal to 9 mm, from which individual bubbles were released from the bottom of an octagonal base tank of side 230 mm and height 500 mm, made in transparent plexiglas, to allow optical access, and filled with still water up to a height of 315 mm. The axis of the steel pipe was placed along the centerline of the tank with the nozzle at 140 mm from the bottom of the tank. The investigated volume extended from the nozzle to 126 mm upward (x-direction), and from -9 mm to 9 mm spanwise (y-direction) and depthwise (z-direction).

The images acquisition system consisted of two couples of Dalsa Falcon 1.4M100 cameras, whose CMOS sensor has a resolution of 1400×1024 pixels at 100 frames per second, equipped with 35 mm focal length lenses, and placed in front of two orthogonal tank sides. It should be noted that the narrow investigated volume allowed to increase the frame rate up to 275 Hz, reducing the frame size to 1400 x 300. The backlight illumination was provided by two LED panels with dimensions 297 mm x 210 mm and power 30 W, placed on the opposite side of the tank with respect to the couples of the camera (Figure 1a).

2.2. Measurement technique

The basic principle of the volumetric shadowgraphy lies upon the evaluation of the air bubbles position, shape, and motion in the three-dimensional space, based on their boundaries observed from different points of view [10, 11]. The projection of each air bubble boundary in the 3D, from the *n* points of view, defines *n* cones having as axis the straight line passing through the optical center of the digital camera lens and the bubble centroid. Figure 1b illustrates the principle, with the projection planes indicated as Oxy and O'x'y', O and O' as optical center and the z-axis as optical axis [10, 11].

The calibration was performed through a planar chessboard (90mm x 50mm) with checkerboard size of 5 mm, leading to an error in the reprojection of the checkerboard corners in the 3D space between -1.5 pixels to 1.5 pixels corresponding to -0.2 mm to 0.2 mm. In addition, the technique was also validated through a series of measurements on polypropylene spheres of known size [10]. Moreover, the detection of the air bubbles boundaries passing from an image processing stage, extensively described in Di Nunno et al. (2020) [10, 11].

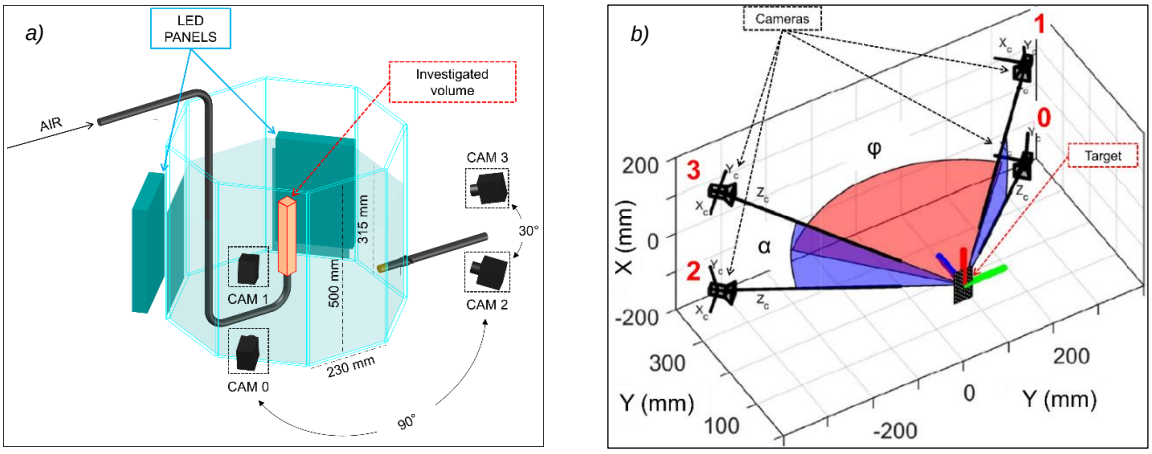

Figure 1. Experimental setup (a); Measurement principle [10] (b).

3. Results and Discussion

The experimental test consisted in the acquisition of a data set containing three in-line air bubbles, released with a time interval between them equal to 0.13 s. The number of frames recorded is equal to 180, recorded at 275 fps. In particular, the first bubble, indicated as *B1*, was recorded into the investigated volume for a time equal to 0.42 s, from frame 1 to frame 127. The second (*B2*) and third (*B3*) bubbles were instead recorded for a time equal to 0.36 s, respectively from frame 36 to frame 146 and from frame 70 to frame 180. Figure 2 shows five non-consecutive frames, recorded with a time interval of 0.04 seconds, which show the evolution of the shape of the three bubbles during their rising.

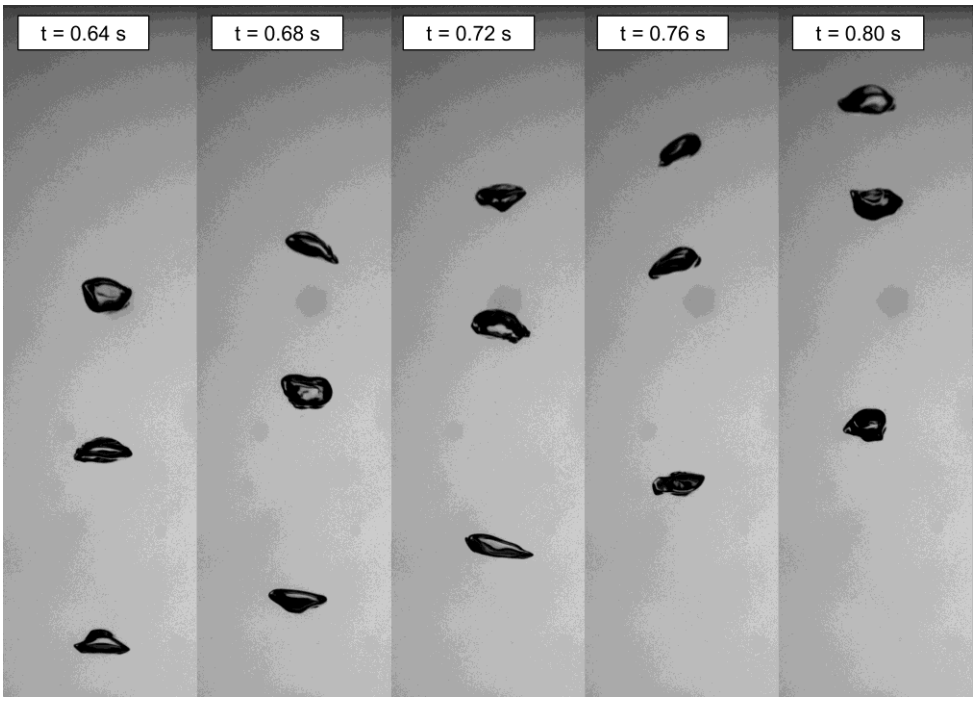

Figure 2. Recorded frames with Cam0: from t = 0.64 s to t = 0.80 s.

A three dimensional representation of the reconstructed air bubbles trajectory, colored as a function of the eccentricity, expressed as the ratio between the minor axis and the major axis, is reported in Figure 3, with also a top view (Plane Y/D – Z/D) of the bubbles. Bubbles followed a spiral like trajectory with a spherical shape (red color, corresponding to an eccentricity of about 0.9) near the outlet section and an elliptical one during their rise, and in particular along the curvatures intervals (blue color, corresponding to the minimum eccentricity of about 0.3). Eccentricity fluctuation were also observed, with a more spherical shape along the straight intervals (green and orange colors, corresponding to an eccentricity between 0.6 and 0.7).

The kinematics and geometric characteristics of the in-line rising bubbles are compared in Figure 4, where the temporal evolution of the dimensionless volume Ψ (dashed line) and dimensionless streamwise velocity U (continuous line), normalized with their respectively maximum value along the time series, are reported for *B1* (Figure 4a), *B2* (Figure 4b), *B3* (Figure 4c). A phase opposition relationship can be noted, with higher oscillation, both in terms of size and velocity, observed for *B2*, for which the U ranged between 0.2 and 1 and Ψ between 0.5 and 1. Bubbles *B1* and *B3* highlighted similar trends, with U that ranged between 0.4 and 1 for *B1* and between 0.3 and 1 for *B3*, Ψ ranged between 0.6 and 1 for both the air bubbles. However, the intensity of the oscillations fades over time, indicating a simultaneous reduction in the effect linked to the release from the steel pipe of the air bubbles.

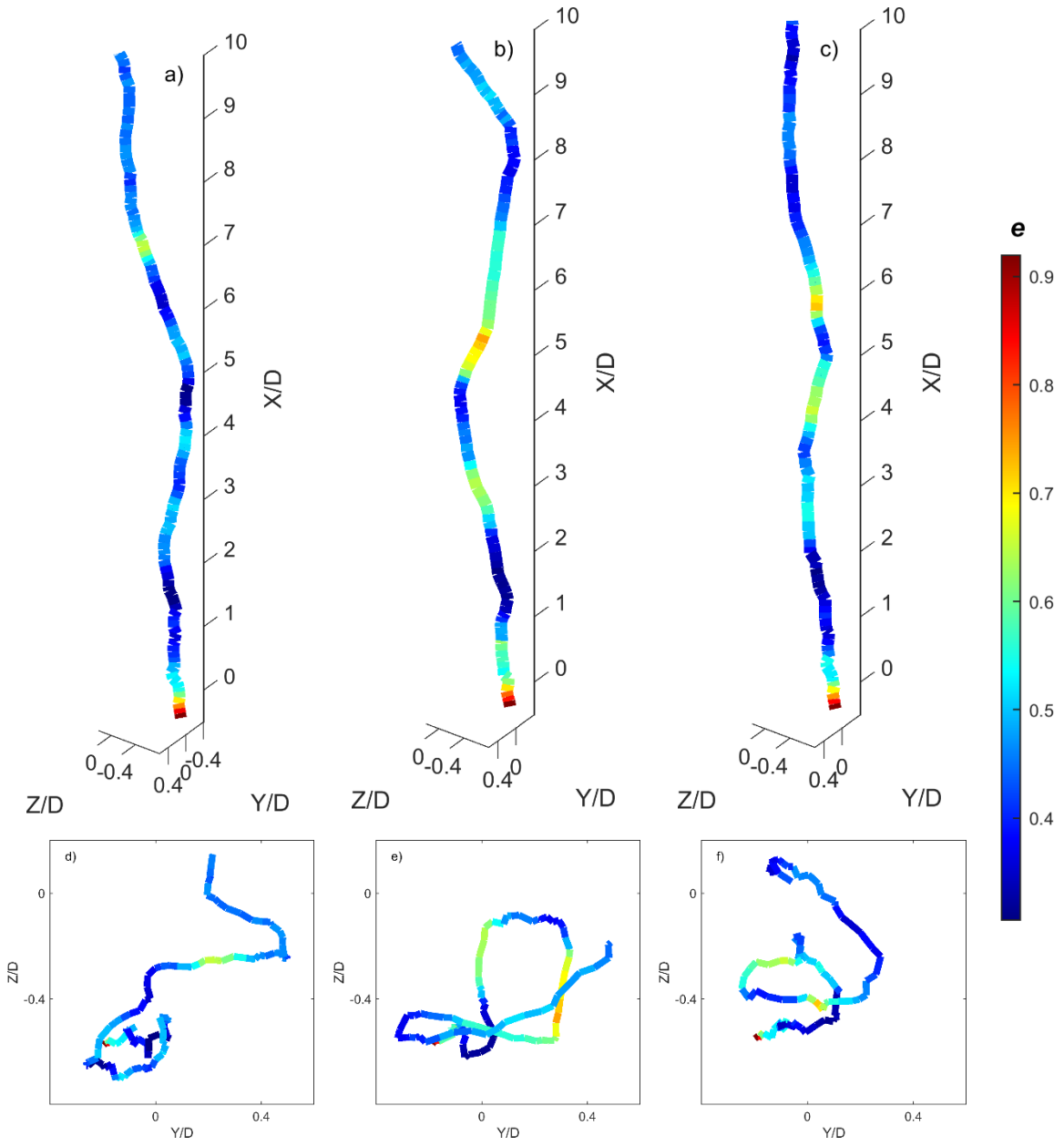

Figure 3. 3D view of the reconstructed air bubbles: *B1* (a); *B2* (b); *B3* (c); view from top: *B1* (d); *B2* (e); *B3* (f).

Moreover, the time evolution of the semi-axes of the equivalent ellipsoid, minor (red), median (green), major (black), together with the bubble eccentricity (dashed line), are reported for *B1* (Figure 5a), *B2* (Figure 5b), *B3* (Figure 5c). The bubbles shape appears more spherical near the release point, showing a more elliptical shape during its rising with fluctuation of the eccentricity values, as observed in Figure 3. Also in this case, a phase opposition relationship can be noted between the minor semi-axis and the two semi-axes median and major, which instead exhibited a similar trend. Overall, their patterns highlighted the existence of an equatorial and almost circular plane, which oscillates in opposition of phase with the orthogonal axis (which corresponds to the direction of the minor semi-axis), in agreement with some literature result [19].

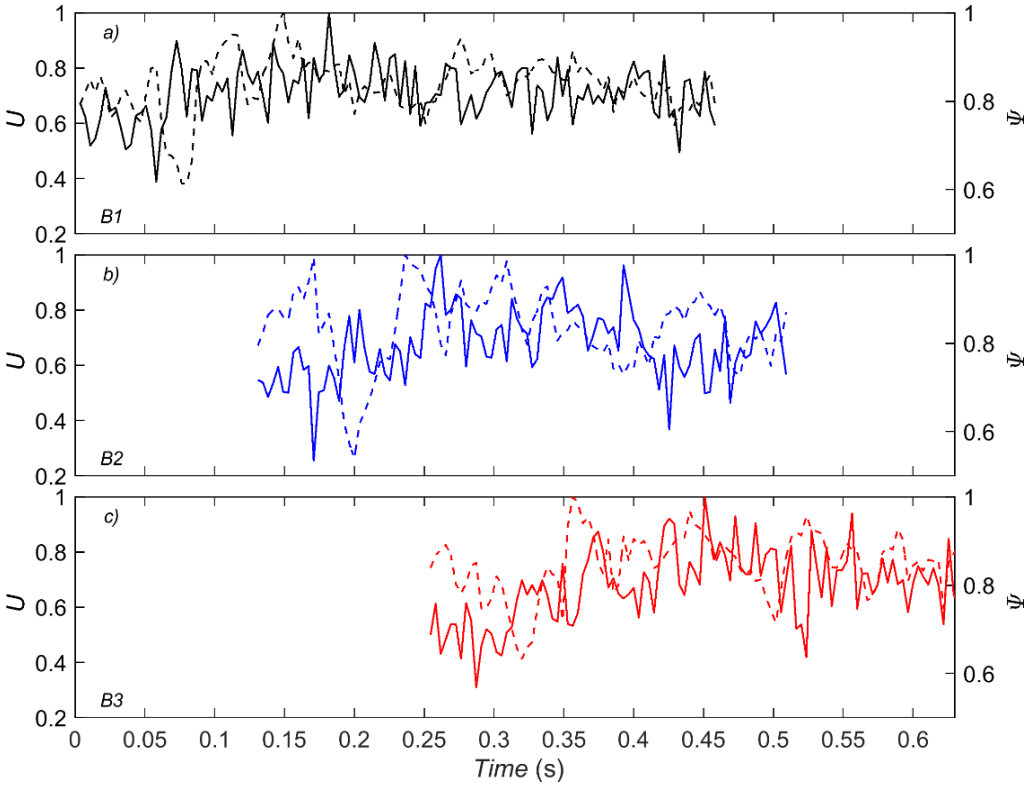

Figure 4. Time evolution of the three in-line bubbles: normalized rising velocity U (continuous line) and normalized volume Ψ for diameters (dashed line).

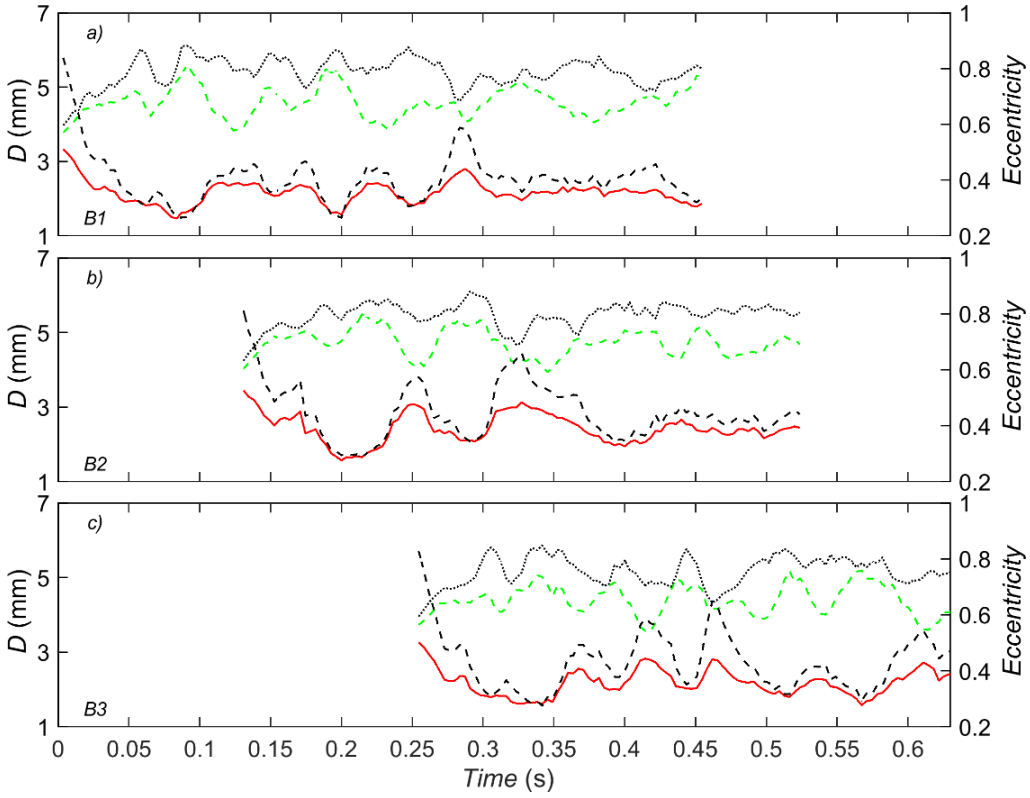

Figure 5. Time evolution of the three in-line bubbles: semi-axis of the equivalent ellipsoid, minor (red line), median (green line), major (black line), together with eccentricity (dashed line).

In order to evaluate the wake characteristics related to the three in-line bubbles, a cross-correlation analysis was carried out by means of cross-correlation function *XCF* computed between the eccentricities of the three bubbles:

$$XCF = \int_0^s e_a(t) \cdot e_b(t+\tau) d\tau$$

where *s* is the size of the time series, $e_a(t)$ and $e_b(t)$ indicates the eccentricities of two different bubbles and τ is the lag [14]. The *XCF* between the eccentricities of *B1* and *B2* (Figure 6a) highlights a peak of 0.4 at 0.2 s, indicating a positive correlation between the two air bubbles. The *XCF* between the eccentricities of *B2* and *B3* (Figure 6b) highlights also a positive peak, slightly lower and equal to 0.35, at 0.16 s but also exhibit a negative peak equal to -0.4 at 0.07 s, indicating a negative correlation, with *B2* that became more spherical when *B3* assumed a flattened shape and vice versa. The *XCF* between the eccentricities of *B1* and *B3* (Figure 6c) highlights also a positive peak, equal to 0.38, at 0.22 s, which is very similar to those observed between *B1* and *B2* (Figure 6a).

A further comparison between the three air bubbles is given in Figure 7, that provide frequency spectra of the time history of the eccentricity, obtained applying the Fourier analysis to the time signal of the eccentricity. Overall, the PSD shows that the eccentricity oscillation frequency was different for the three air bubbles with, however, some common features. The first bubble *B1* highlighted two peaks, the first for a frequency *f* = 6.5 Hz and the second, slightly lower, for *f* = 10.8 Hz. Bubble *B2* exhibited mainly one peak, which was however the highest among the three bubbles, for *f* = 5 Hz. For Bubble *B3* instead two peaks were computed, the first for a frequency *f* = 4.9 Hz, very similar to that computed for *B2*, and a second for *f* = 9.9 Hz, which instead was similar for the second computed for *B1*.

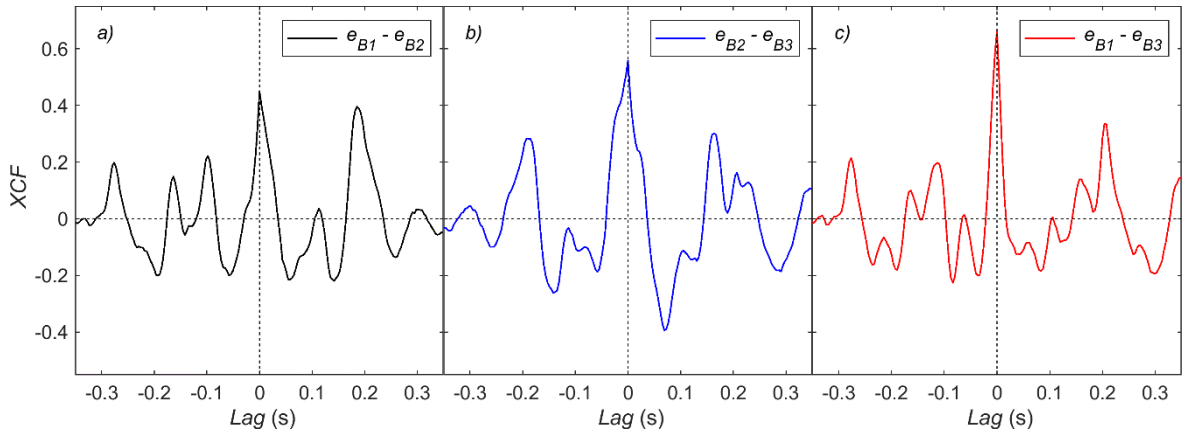

Figure 6. Cross-correlation function between the eccentricities of *B1* and *B2* (a); *B2* and *B3* (b) and *B1* and *B3* (c).

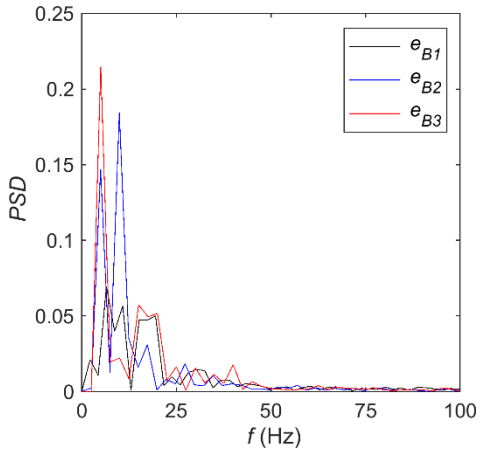

Figure 7. Frequency spectra of eccentricity for the three bubbles.

The *XCF* between the rising velocities of the three bubbles were also computed, expressed as:

$$XCF = \int_0^s U_a(t) \cdot U_b(t+\tau)d\tau$$

where $U_a(t)$ and $U_b(t)$ indicates the rising velocities of two different bubbles. Cross-correlation between the rising velocities of *B1* and *B2* (Figure 8a) exhibits a negative peak of -0.27 at 0. 12 s, with *B2* that slowing down when *B1* accelerates and vice versa. A positive correlation, with a lower peak of 0.17, was instead observed at 0.28 s. Also between *B2* and *B3* (Figure 8b) a negative peak was observed, slightly lower than that computed between *B1* and *B2*, equal to -0.21, and for a higher delay, equal to 0.17 s. The latter was in agreement with the *XCF* between the rising velocities of *B1* and *B3* (Figure 8c) that also highlighted a negative peak at 0.17 s, slightly higher and equal to -0.24.

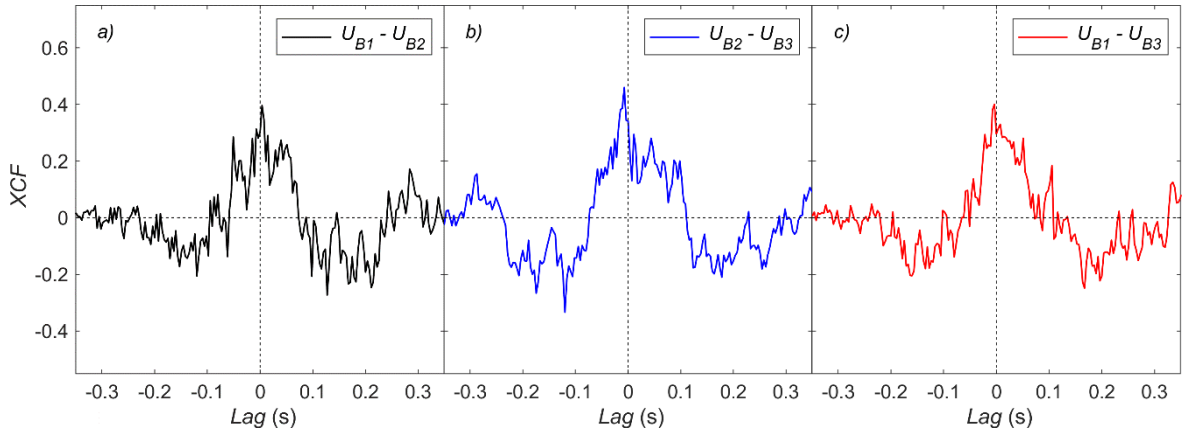

Figure 8. Cross-correlation function between the rising velocities of *B1* and *B2* (a); *B2* and *B3* (b) and *B1* and *B3* (c).

4. Conclusions

An experimental investigation on a sequence of three in-line rising bubbles has been presented. In order to allow a 3D analysis of the air bubbles, a volumetric shadowgraphy technique has been used, which allows to describe the spatio-temporal evolution of the air bubbles inside the investigated volume.
Results show a phase opposition relationship between the volumes and rising velocities of the three air bubbles with more marked oscillation for the intermediate bubbles. A further phase opposition was observed between the minor semi-axis and the two semi-axes median and major for the three bubbles, highlighted the existence of an equatorial and almost circular plane, which oscillates in opposition of phase with the orthogonal axis. The cross-correlation function applied on the eccentricities of the three bubbles highlighted similar positive peaks but also a negative peak between eccentricities of the second and third bubbles, with *B2* that became more spherical when *B3* assumed a flattened shape and vice versa. Moreover, the frequency spectra of the three bubbles eccentricities exhibited some common features, with peaks around 10 Hz for the first and third bubbles and around 5 Hz for the second and third bubbles. Furthermore, the cross-correlation applied on the rising velocities exhibited similar negative correlations between the three bubbles, with each bubble that reduces its rising velocity while another accelerates. Overall, the application of the volumetric shadowgraphy allowed simultaneous measurement of the geometry and rising velocities of the in-line bubbles, leading to identify common and different features among them.

Acknowledgments

The work described here was conducted as part of the Italian Ministry of Education, University and Research 2017 PRIN Project ACE, grant 2017RSH3JY.

5. References

[1] Gumulya M Utikar R P Evans G Joshi J B and Pareek V 2017 Interaction of bubbles rising inline in quiescent liquid *Chem. Eng. Sci.* **166** doi: 10.1016/j.ces.2017.03.013.

[2] Celata G P Cumo M D'Annibale F and Tomiyama A 2004 The wake effect on bubble rising velocity in one-component systems *Int. J. Multiph. Flow* **30**(7-8) pp 939-961 doi: 10.1016/j.ijmultiphaseflow.2004.04.007.
[3] Marks C H 1973 Measurements of the terminal velocity of bubbles rising in a chain *J. Fluid. Eng.* **95**(1) pp 17-22 doi: 10.1115/1.3446951.
[4] Katz J Menevau C 1996 Wake-induced relative motion of bubbles rising in line *Int. J. Multiph. Flow* **22**(2) pp 239-258 doi: 10.1016/0301-9322(95)00081-X.
[5] Sene K 1988 Air entrainment by plunging jets *Chem. Eng. Sci.* **43**(10) pp 2615-2623 doi: 10.1016/0009-2509(88)80005-8.
[6] Chanson H Aoki S and Hoque A 2004 Physical modelling and similitude of air bubble entrainment at vertical circular plunging jets *Chem. Eng. Sci.* **59**(4) pp 747-758 doi: 10.1016/j.ces.2003.11.016.
[7] Xu W Chen C and Wei W 2018 Experimental Study on the Air Concentration Distribution of Aerated Jet Flows in a Plunge Pool *Water*, **10**(12) p 1779 doi: 10.3390/w10121779.
[8] Di Nunno F Alves Pereira F de Marinis G Di Felice F Gargano R Granata F and Miozzi M 2019 Two-phase PIV-LIF measurements in a submerged bubbly water jet *J. Hydraul. Eng.* **145**(9) doi: 10.1061/(ASCE)HY.1943-7900.0001620.
[9] Di Nunno F Alves Pereira F de Marinis G Di Felice F Gargano R Granata F and Miozzi M 2018 Experimental study of air-water two-phase jet: Bubble size distribution and velocity measurements *J. Phys. Conf. Ser.* **1110** doi: 10.1088/1742-6596/1110/1/012011.
[10] Di Nunno F Granata F de Marinis G Di Felice F Gargano R and Miozzi M 2020 A shadowgraphy approach for the 3D Lagrangian description of bubbly flows *Meas. Sci. Technol.*, **31**(10) doi: 10.1088/1361-6501/ab8fef.
[11] Di Nunno F Alves Pereira F Miozzi M Granata F Gargano R de Marinis G and 2020 Experimental study of a vertical plunging jet by means of a volumetric shadowgraph technique *J. Phys. Conf. Ser.* **1589** doi: 10.1088/1742-6596/1589/1/012006.
[12] Granata F Di Nunno F Gargano R and de Marinis G 2019 Equivalent Discharge Coefficient of Side Weirs in Circular Channel-A Lazy Machine Learning Approach *Water* **11**(11) doi: 10.3390/w11112406.
[13] Di Nunno F Alves Pereira F de Marinis G Di Felice F Gargano R Miozzi M and Granata F 2020 Deformation of Air Bubbles Near a Plunging Jet Using a Machine Learning Approach *Applied Science* **10**(11) doi: 10.3390/app10113879.
[14] Iannello J P 1982 Time delay estimation via cross-correlation in the presence of large estimation errors *IEEE Trans. Signal Process.***30**(6) pp 998-1003 doi: 10.1109/tassp.1982.1163992.